

Deducing the nature of dark matter from direct and indirect detection experiments in the absence of collider signatures of new physics

Maria Beltran

Department of Astronomy and Astrophysics, The University of Chicago

Dan Hooper

*Theoretical Astrophysics, Fermi National Accelerator Laboratory and
Department of Astronomy and Astrophysics, The University of Chicago*

Edward W. Kolb

*Department of Astronomy and Astrophysics, Enrico Fermi Institute,
and Kavli Institute for Cosmological Physics, The University of Chicago*

Zosia A. C. Krusberg

Department of Physics, The University of Chicago

Despite compelling arguments that significant discoveries of physics beyond the standard model are likely to be made at the Large Hadron Collider, it remains possible that this machine will make no such discoveries, or will make no discoveries directly relevant to the dark matter problem. In this article, we study the ability of astrophysical experiments to deduce the nature of dark matter in such a scenario. In most dark matter studies, the relic abundance and detection prospects are evaluated within the context of some specific particle physics model or models (e.g., supersymmetry). Here, assuming a single weakly interacting massive particle constitutes the universe's dark matter, we attempt to develop a model-independent approach toward the phenomenology of such particles in the absence of any discoveries at the Large Hadron Collider. In particular, we consider generic fermionic or scalar dark matter particles with a variety of interaction forms, and calculate the corresponding constraints from and sensitivity of direct and indirect detection experiments. The results may provide some guidance in disentangling information from future direct and indirect detection experiments.

PACS numbers: 95.35.+d;95.30.Cq;95.85.Ry;95.55.Ka; FERMILAB-PUB-08-308-A

I. INTRODUCTION

The consensus of the astrophysics community is that a large fraction of the universe's mass consists of non-luminous, non-baryonic material, known as dark matter [1]. Although the nature of this substance or substances remains unknown, weakly interacting massive particles (WIMPs) represent a particularly attractive and well motivated class of possibilities. Although the most studied WIMP candidate is the lightest neutralino [2] in supersymmetric models, many other possibilities have also been proposed, including Kaluza-Klein states in models with universal [3, 4] or warped [5] extra dimensions, stable states in Little Higgs theories [6], and many others.

In each of the above mentioned cases, many new particle species, in addition to the WIMP itself, are expected to lie within the discovery reach of the Large Hadron Collider (LHC), making the task of deducing the nature of the WIMP immeasurably simpler. In supersymmetry, for example, gluinos and squarks are expected to be produced prolifically. By studying the cascades produced in the decays of such particles, the masses of several superparticle masses, including the lightest neutralino, are likely to be determined. If squarks, gluinos, and other additional superpartners are too heavy to be produced, however, the lightest neutralino will also be very difficult to study at the LHC, even if rather light itself. More generally speaking, in the absence of heavier particles with shared quantum numbers, WIMPs will not be easily detected or studied at the LHC. Although an electroweak scale, cold thermal relic particle, if it exists, would almost certainly be produced at the LHC, identifying and characterizing the nature of the WIMP simply from missing energy studies is a daunting, perhaps impossible, task [7, 8].

Although the usual list of prospective WIMPs mentioned above contains some very attractive and well-motivated candidates for dark matter, there are certainly many possible forms of dark matter that have not yet been considered. As the first observations of particle dark matter might well come from direct and/or indirect detection experiments, it is possible that these results may be misinterpreted as a result of theoretical bias, anticipating dark matter to have the properties of a neutralino or other often studied candidates. To avoid such confusion, model-independent studies of dark matter phenomenology can play an important role (for previous work in this direction, see Refs. [7, 9, 10]).

In this article, rather than consider a WIMP candidate from a specific theoretical model, we study model-

independent WIMPs with different combinations of spins and interaction forms with standard model particles. These interactions are limited only by the requirements of Lorentz invariance and a consequent WIMP abundance consistent with cosmological observations. For each spin and interaction form, we evaluate the constraints from and prospects for direct and indirect detection of WIMPs in current and future experiments. Although we will be forced to adopt some assumptions in order to make the problems at hand tractable, we attempt to be as general as possible throughout our study. Beyond the starting point that the dark matter is a WIMP in the form of a single species of a cold thermal relic, we adopt only two assumptions:

1. Any new particle species in addition to the WIMP has a mass much larger than the WIMP.
2. The WIMP interactions with standard model particles are dominated by those of one form (scalar, vector, *etc.*).

An implication of the first assumption is that the WIMP's thermal abundance is not affected by resonances or coannihilations. At a later stage of this paper, we will discuss the impact of relaxing these assumptions.

The remainder of this paper is structured as follows. In Sec. II we explore the phenomenology of a generic fermionic WIMP, including its annihilation cross section and relic abundance, elastic scattering cross section and direct detection prospects, and indirect detection prospects in the form of a neutrino flux from the Sun and gamma rays and charged particles produced in galactic annihilations. In Sec. III, we repeat this exercise for the case of a scalar WIMP. In each of these two sections, we also consider dark matter candidates from specific particle physics frameworks and discuss how they fit into our model-independent analysis. In Sec. IV we summarize our results and present our conclusions.

II. FERMIONIC DARK MATTER

We begin with the case of a fermionic WIMP, and study five types of interactions consistent with the requirement of Lorentz invariance. As mentioned in the Introduction, we assume that the WIMP is the only new particle at the electroweak scale. This enables us to describe the interaction between WIMPs and standard model fermions in terms of an effective field theory, in which we keep only the first term in the $(q/M)^2$ expansion of the heavy propagator term (here, q and M are the momentum and mass of the propagator, respectively). We note that the effective interaction Lagrangians are not invariant under the standard model $SU(2)_W \times U(1)_Y$ gauge symmetry; however, this is acceptable as our theory need only be valid at energy scales below the scale of electroweak symmetry breaking.

To begin, we only consider WIMP annihilations to fermion-antifermion pairs, neglecting for the moment the possibility of final states that include gauge or Higgs bosons. In particular, we consider the following interaction Lagrangians between two fermionic WIMPs (χ) and two standard model fermions (f):

$$\text{Scalar (S): } \mathcal{L} = \frac{G_S}{\sqrt{2}} \bar{\chi} \chi \bar{f} f \quad (1)$$

$$\text{Pseudoscalar (P): } \mathcal{L} = \frac{G_P}{\sqrt{2}} \bar{\chi} \gamma^5 \chi \bar{f} \gamma_5 f \quad (2)$$

$$\text{Vector (V): } \mathcal{L} = \frac{G_V}{\sqrt{2}} \bar{\chi} \gamma^\mu \chi \bar{f} \gamma_\mu f \quad (3)$$

$$\text{Axial Vector (A): } \mathcal{L} = \frac{G_A}{\sqrt{2}} \bar{\chi} \gamma^\mu \gamma^5 \chi \bar{f} \gamma_\mu \gamma_5 f \quad (4)$$

$$\text{Tensor (T): } \mathcal{L} = \frac{G_T}{\sqrt{2}} \bar{\chi} \sigma^{\mu\nu} \chi \bar{f} \sigma_{\mu\nu} f. \quad (5)$$

We will now proceed to calculate the annihilation cross section, relic density, and elastic scattering cross sections for a fermionic WIMP.

A. Fermionic WIMP Annihilation and Relic Density

In each of the cases listed above, we are interested in determining the cosmological density of WIMPs produced in the early universe. The first step is to calculate the annihilation cross sections to fermion-antifermion pairs as a

function of the Mandelstam variable s for each of the five cases. The result is

$$\sigma_S = \frac{1}{32\pi} \sum_f G_{S,f}^2 c_f \sqrt{\frac{s-4m_f^2}{s-4M_\chi^2}} \left[\frac{(s-4M_\chi^2)(s-4m_f^2)}{s} \right] \quad (6)$$

$$\sigma_P = \frac{1}{32\pi} \sum_f G_{P,f}^2 c_f \sqrt{\frac{s-4m_f^2}{s-4M_\chi^2}} s \quad (7)$$

$$\sigma_V = \frac{1}{32\pi} \sum_f G_{V,f}^2 c_f \sqrt{\frac{s-4m_f^2}{s-4M_\chi^2}} \left[s + 4M_\chi^2 + \frac{(s-4M_\chi^2)(s-4m_f^2)}{3s} + 4m_f^2 \right] \quad (8)$$

$$\sigma_A = \frac{1}{32\pi} \sum_f G_{A,f}^2 c_f \sqrt{\frac{s-4m_f^2}{s-4M_\chi^2}} \left[s - 4M_\chi^2 + \frac{(s-4M_\chi^2)(s-4m_f^2)}{3s} + 4m_f^2 \right] \quad (9)$$

$$\sigma_T = \frac{1}{32\pi} \sum_f G_{T,f}^2 c_f \sqrt{\frac{s-4m_f^2}{s-4M_\chi^2}} \left[6s + 4M_\chi^2 + \frac{8(s-4M_\chi^2)(s-4m_f^2)}{3s} + 4m_f^2 \right] \quad (10)$$

where the sum is over the final state fermion species and c_f are the color factors, equal to 3 for quarks and 1 for leptons.

To determine the density of relic WIMPs, we solve the Boltzmann equation:

$$\frac{dn_\chi}{dt} + 3Hn_\chi = -\langle\sigma|v\rangle [(n_\chi)^2 - (n_\chi^{\text{eq}})^2], \quad (11)$$

where $H \equiv \dot{a}/a = \sqrt{8\pi\rho/3M_{\text{Pl}}}$ is the Hubble rate and $\langle\sigma|v\rangle$ is the thermally averaged WIMP annihilation cross section [11].

In thermal equilibrium, the number density of WIMPs is given by:

$$n_\chi^{\text{eq}} = g \left(\frac{M_\chi T}{2\pi} \right)^{3/2} \exp\left(-\frac{M_\chi}{T}\right), \quad (12)$$

where $g = 2$ is the number of degrees of freedom of a fermionic WIMP. At $T \gg M_\chi$, the number density of WIMPs was very close to its equilibrium value and nearly as abundant as any other particle. As the temperature dropped below M_χ , however, the number density was exponentially suppressed until, eventually, the annihilation and production rates became much smaller than the expansion rate, and the species froze out of equilibrium. Since we are considering cold thermal relics, freeze-out occurred when WIMPs were non-relativistic and had velocities much smaller than unity. Substituting $s \approx 4M_\chi^2 + M_\chi^2 v^2$ to Eqs. (6-10), and expanding in powers of the relative velocity between two annihilating WIMPs up to order v^2 , we find

$$\sigma_S|v| \approx \frac{1}{4\pi} \sum_f G_{S,f}^2 c_f M_\chi^2 \sqrt{1-m_f^2/M_\chi^2} \left[\frac{1}{4} \left(1 - \frac{m_f^2}{M_\chi^2} \right) v^2 \right] \quad (13)$$

$$\sigma_P|v| \approx \frac{1}{4\pi} \sum_f G_{P,f}^2 c_f M_\chi^2 \sqrt{1-m_f^2/M_\chi^2} \quad (14)$$

$$\sigma_V|v| \approx \frac{1}{4\pi} \sum_f G_{V,f}^2 c_f M_\chi^2 \sqrt{1-m_f^2/M_\chi^2} \left[\left(2 + \frac{m_f^2}{M_\chi^2} \right) + \frac{1}{12} \left(1 - \frac{m_f^2}{M_\chi^2} \right) v^2 \right] \quad (15)$$

$$\sigma_A|v| \approx \frac{1}{4\pi} \sum_f G_{A,f}^2 c_f M_\chi^2 \sqrt{1-m_f^2/M_\chi^2} \left[\frac{m_f^2}{M_\chi^2} + \frac{1}{12} \left(2 - \frac{m_f^2}{M_\chi^2} \right) v^2 \right] \quad (16)$$

$$\sigma_T|v| \approx \frac{1}{4\pi} \sum_f G_{T,f}^2 c_f M_\chi^2 \sqrt{1-m_f^2/M_\chi^2} \left[\left(7 + \frac{m_f^2}{M_\chi^2} \right) + \frac{2}{3} \left(1 - \frac{m_f^2}{M_\chi^2} \right) v^2 \right]. \quad (17)$$

Numerical solutions of the Boltzmann equation yield a relic density of [12]:

$$\Omega_\chi h^2 \approx \frac{1.04 \times 10^9 x_F}{M_{\text{Pl}} \sqrt{g_*} (a + 3b/x_F)}, \quad (18)$$

where $x_F = m_\chi/T_F$, T_F is the temperature at freeze-out, g_* is the number of relativistic degrees of freedom available at freeze-out ($g_* \approx 92$ for a freeze-out temperature between the bottom quark and W boson masses), and a and b are terms in the partial wave expansion of the WIMP annihilation cross section, $\sigma|v| = a + bv^2 + \mathcal{O}(v^4)$. Evaluation of x_F leads to

$$x_F = \ln \left[c(c+2) \sqrt{\frac{45}{8}} \frac{g M_\chi M_{\text{Pl}} (a + 6b/x_F)}{2\pi^3 \sqrt{g_*(x_F)}} \right], \quad (19)$$

where c is an order unity parameter determined numerically. WIMPs with electroweak-scale masses and couplings generically freeze out at temperatures in the range of approximately $x_F \approx 20$ to 30.

In the absence of resonances and coannihilations [13], an annihilation cross section of $\langle \sigma|v| \rangle \sim 3 \times 10^{-26} \text{ cm}^3/\text{s} \approx 1 \text{ pb}$ is required (at the temperature of freeze-out, $T \sim m_\chi/20$) to obtain a relic abundance in agreement with the dark matter abundance measured by WMAP, $\Omega_\chi h^2 = 0.1099 \pm 0.0062$ [14]. Although the annihilation cross section in the low-velocity limit (relevant to indirect dark matter searches) is not much lower than this value in many models, it can be considerably suppressed at low velocities if terms in the annihilation cross section proportional to v^2 dominate the cross section (*i.e.*, if $a \ll b$). Furthermore, if the depletion of WIMPs in the early universe occurs through resonance channels or via coannihilations with other states, the low velocity annihilation cross section can be considerably lower than the value at freeze-out. For more details regarding the relic density calculation, see Refs. [12, 13].

In Fig. 1, we show the thermal relic density of a fermionic dark matter candidate with scalar, pseudoscalar, vector, and axial interactions. We do not include a separate figure for the tensor case, since its annihilation cross section is nearly identical to the vector case. As discussed in the Introduction, these results were found under the assumptions that a given WIMP's interactions are dominated by those of only one form (scalar, vector, *etc.*), that the WIMP's interactions are mediated by particles much heavier than the WIMP mass (thus avoiding the possibility of resonance effects), and that the WIMP is considerably lighter than any other new particles (thus making coannihilations unimportant). Also, we include only annihilations to fermion-antifermion pairs (neglecting the possibility of final states including gauge or Higgs bosons).

In each frame of Fig. 1, we show the relic density for various values of the effective couplings. In the upper left and upper right frames, we show results for couplings of $G_f \times (1 \text{ GeV}/m_f) = 10^{-8}, 10^{-7}, 10^{-6}, 10^{-5}$, and 10^{-4} GeV^{-2} . This proportionality of the couplings to the fermion mass is predicted for Yukawa couplings of a Higgs mediated interaction, for example. In the remaining four frames, we show results for the case of universal couplings, $G_f = 10^{-8}, 10^{-7}, 10^{-6}, 10^{-5}$, and 10^{-4} GeV^{-2} .

If any of our assumptions are broken, the resulting thermal relic abundance will be altered as well. In particular, resonances (or more generally, a departure from $2M_\chi \ll M_\psi$) or coannihilations could potentially reduce the abundances shown in Fig. 1 considerably. Additionally, annihilations to final states such as gauge or Higgs bosons, if significant, could also reduce the relic density. The effective couplings described in Fig. 1 that lead to the correct relic abundance, therefore, can be thought of as approximate maximal values allowed for a thermal WIMP.¹ Smaller couplings are possible if appropriate departures are made from our set of assumptions.

B. Direct Detection

Although only weakly coupled to baryons, WIMPs can occasionally scatter elastically with atomic nuclei, providing the potential for detection. Direct detection experiments attempt to measure the recoil energies of nuclei resulting from such interactions. The interactions leading to the elastic scattering of WIMPs with nuclei can be classified as either spin-independent or spin-dependent. In the former case, WIMPs scatter coherently with an entire nucleus, leading to a cross section that scales with the square of the atomic number of the target nuclei. In the later case, the WIMP couples to the spin of the target nucleus. In the relevant non-relativistic limit, scalar, vector, and tensor couplings result in a spin-independent interaction, whereas axial couplings lead to a spin-dependent interaction [15]. In this subsection, we focus on the spin-independent elastic scattering of WIMPs with nuclei, as the direct detection constraints for this class of interactions are considerably more stringent. In the next subsection, we will return to spin-dependent scattering within the context of WIMP capture in the Sun.

¹ Larger couplings may be possible if the density of WIMPs is enhanced by post-freezeout decays of other particles or other non-thermal production mechanisms. For example, see [4].

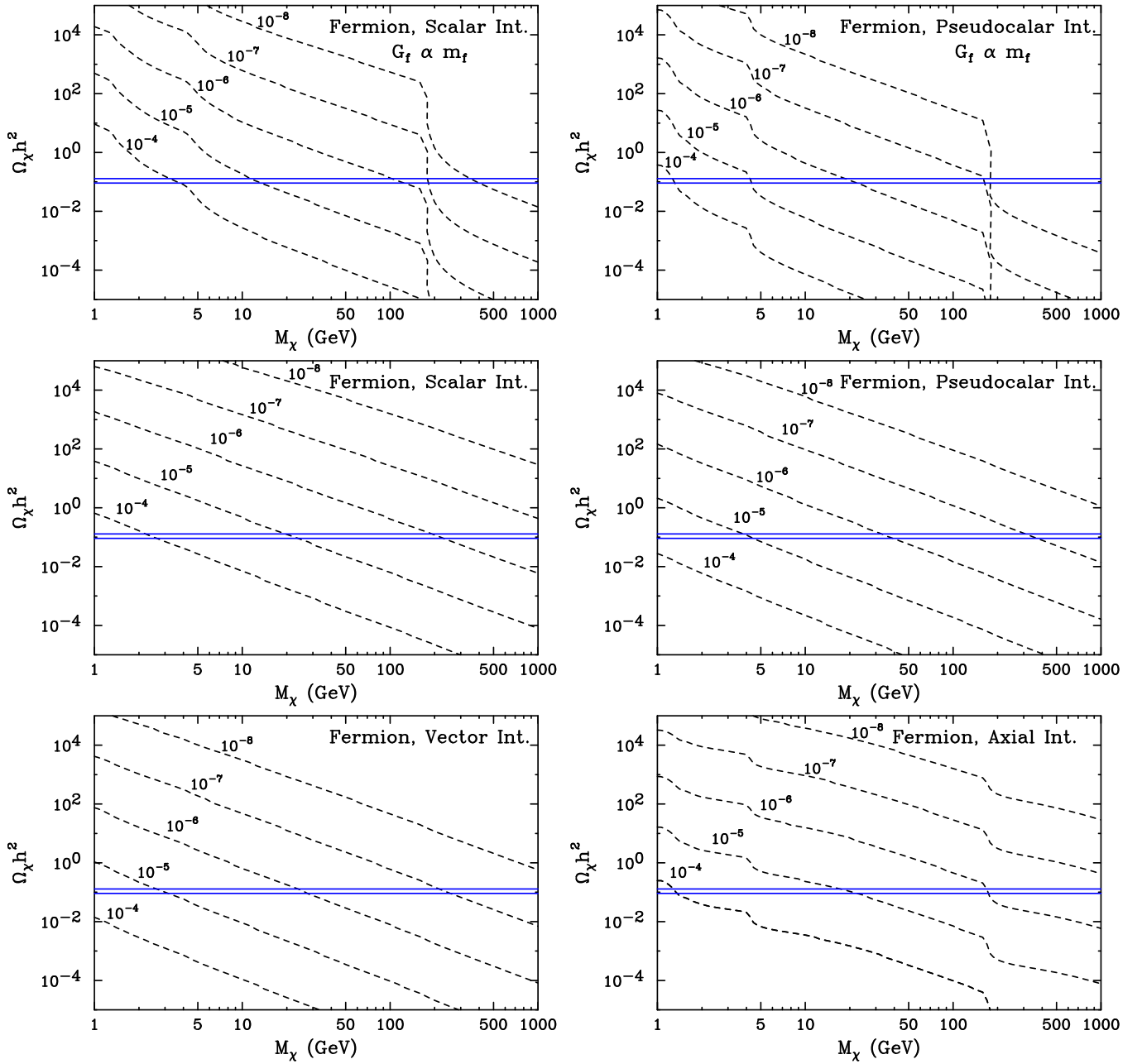


FIG. 1: The thermal relic density of fermionic dark matter with scalar, pseudoscalar, vector, and axial interactions. In the upper left and upper right frames, results are given for effective couplings to each species of standard model fermion of $G_f \times (1 \text{ GeV}/m_f) = 10^{-8}, 10^{-7}, 10^{-6}, 10^{-5},$ and 10^{-4} GeV^{-2} . In the remaining four frames, results are shown for $G_f = 10^{-8}, 10^{-7}, 10^{-6}, 10^{-5},$ and 10^{-4} GeV^{-2} . If resonances, coannihilations, or annihilations to final states other than fermion-antifermion pairs are significant, the relic abundance is expected to be significantly lower than shown here. Also shown as horizontal lines is the range of the cold dark matter density measured by WMAP [14].

The WIMP-nucleus cross section for spin-independent elastic scattering is given by

$$\sigma_{\chi N} = \frac{4}{\pi} \frac{M_\chi^2 m_N^2}{(M_\chi + m_N)^2} [Z f_p + (A - Z) f_n]^2 \quad (20)$$

where A and Z are the atomic mass and atomic number of the target nuclei. The effective couplings to protons and

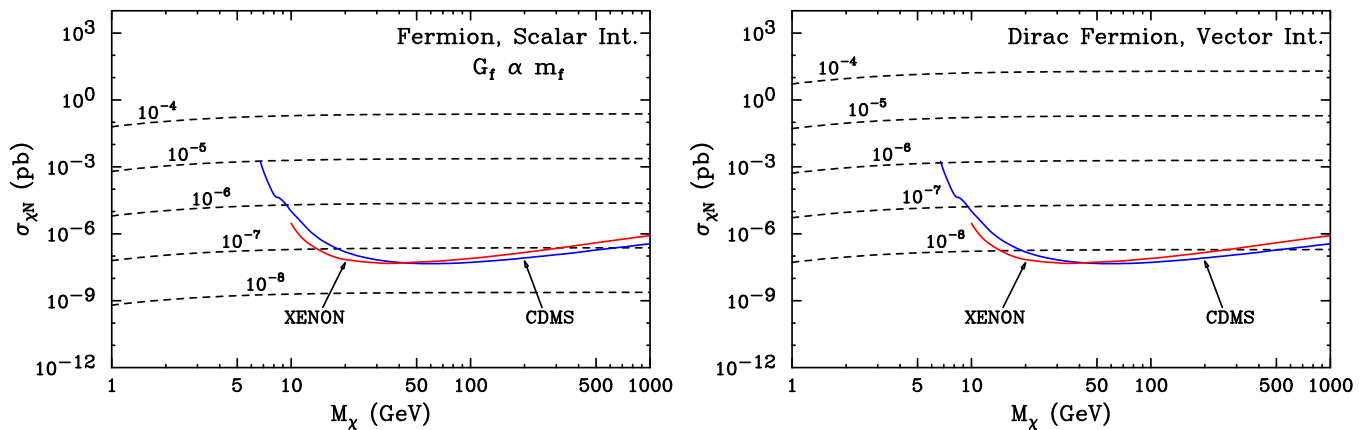


FIG. 2: The spin-independent WIMP-nucleon elastic scattering cross section as a function of WIMP mass for a fermionic WIMP interacting through scalar (left) and vector (right) interactions. Results are given for effective scalar couplings to each quark species of $G_q \times (1 \text{ GeV}/m_q) = 10^{-8}, 10^{-7}, 10^{-6}, 10^{-5},$ and 10^{-4} GeV^{-2} and for effective vector couplings to each quark of $G_q = 10^{-8}, 10^{-7}, 10^{-6}, 10^{-5},$ and 10^{-4} GeV^{-2} . Also shown as solid curves are the current upper limits from the CDMS [17] and XENON [18] experiments. We do not show the case in which the scalar couplings are equal for each quark species, as its leads to much larger cross sections and are strongly excluded.

neutrons, $f_{p,n}$, can be written in terms of the WIMP's couplings to quarks. In the case of a scalar interaction

$$f_{p,n} = \sum_{q=u,d,s} \frac{G_q}{\sqrt{2}} f_{Tq}^{(p,n)} \frac{m_{p,n}}{m_q} + \frac{2}{27} f_{TG}^{(p,n)} \sum_{q=c,b,t} \frac{G_q}{\sqrt{2}} \frac{m_{p,n}}{m_q}, \quad (21)$$

where G_q denotes the WIMP's effective Fermi coupling for a given quark species. The first term reflects scattering with light quarks, while the second term accounts for interactions with gluons through a heavy quark loop. The values of $f_{Tq}^{(p,n)}$ are proportional to the matrix element, $\langle \bar{q}q \rangle$, of quarks in a nucleon and have been measured to be $f_{Tu}^p = 0.020 \pm 0.004$, $f_{Td}^p = 0.026 \pm 0.005$, $f_{Ts}^p = 0.118 \pm 0.062$, $f_{Tu}^n = 0.014 \pm 0.003$, $f_{Td}^n = 0.036 \pm 0.008$, $f_{Ts}^n = 0.118 \pm 0.062$ [16]. The value of $f_{TG}^{(p,n)}$ is given by $f_{TG}^{(p,n)} = 1 - \sum_{u,d,s} f_{Tq}^{(p,n)}$ and is approximately 0.84 and 0.83 for protons and neutrons, respectively.

In the case of a Yukawa-like scalar interaction ($G_q \propto m_q$), there are significant contributions from both light and heavy quarks. In the case in which the ratio of the effective scalar coupling to the quark mass, $G_{S,q}/m_q$, is the same for each quark species, we arrive at a cross section per nucleon of

$$\sigma_{\chi,p} \approx 3 \times 10^{-7} \text{ pb} \times \left[\frac{G_{S,q} \times (1 \text{ GeV}/m_q)}{10^{-7} \text{ GeV}^{-2}} \right]^2. \quad (22)$$

In contrast, if we consider the case in which the scalar couplings to all quarks types are equal (universal couplings), the resulting cross section is much larger:

$$\sigma_{\chi,p} \sim 3 \times 10^{-4} \text{ pb} \times \left(\frac{G_{S,q}}{10^{-7} \text{ GeV}^{-2}} \right)^2. \quad (23)$$

The cross section for the scalar case of $G_q \propto m_q$ is shown in the left frame of Fig. 2, and compared to the current upper limits from the CDMS [17] and XENON [18] experiments. For fermionic WIMPs heavier than about 10 GeV, scalar couplings are constrained to be smaller than $G_{S,q} \times (1 \text{ GeV}/m_q) \sim 10^{-7}$. Comparing this result to those shown in Fig. 1, we find that fermionic WIMPs must either be heavier than the top quark threshold to avoid being overproduced in the early universe *and* avoid direct detection constraints *or* some combination of resonance annihilation, coannihilation, or annihilations to final states other than quarks must dominate the thermal freeze-out process.

If instead we were to consider the case of universal scalar couplings to all quark types, as applied in Eq. (23), we find an even more stringent constraint. In particular, the entire range of couplings that could potentially lead to an acceptable relic density is excluded by current direct detection constraints by multiple orders of magnitude. We therefore conclude that if a WIMP is to annihilate largely through scalar interactions, its couplings to light quarks

must be considerably suppressed (such as in the case of Yukawa-like couplings, $G_f \propto m_f$) if it is to avoid being excluded by current direct detection constraints.

In contrast to scalar interactions, pseudoscalar interactions do not lead to a significant elastic scattering cross section between WIMPs and nucleons in the low velocity limit. The reason for this can be seen if one explicitly computes the quark contribution of the vertex, $\bar{q}\gamma_5 q$, which goes to zero in the limit of zero momentum [19]. The same conclusion is reached in Ref. [10], in which the relevant nuclear matrix elements are calculated.

In the case of a Dirac (non-Majorana) fermion, a vector coupling can also generate a spin-independent elastic scattering cross section. In contrast to the scalar case, a vector interaction will be dominated by couplings to the up and down quarks in the nucleon:

$$f_p = 2 \frac{G_{V,u}}{\sqrt{2}} + \frac{G_{V,d}}{\sqrt{2}}, \quad f_n = \frac{G_{V,u}}{\sqrt{2}} + 2 \frac{G_{V,d}}{\sqrt{2}}. \quad (24)$$

If we assume $G_{V,u} \approx G_{V,d}$, this leads to a spin-independent elastic scattering cross section (per nucleon) of $\sigma_{\chi,p} \approx 2 \times 10^{-5} \text{ pb} \times (G_V/10^{-7} \text{ GeV}^{-2})^2$. From the right frame of Fig. 2, we see that this cross section is in excess of current experimental limits [17, 18] unless $G_V \lesssim 10^{-8} \text{ GeV}^{-2}$. Comparing this to Fig. 1, however, we find that in order for a Dirac fermionic WIMP with a mass in the range 10 to 1000 GeV to annihilate largely through a vector interaction, it must be depleted in the early universe by some combination of resonance annihilation, coannihilation, or annihilations to final states other than quarks if it is to avoid direct detection constraint without being overproduced in the early universe. This conclusion also holds for a fermionic WIMP with a tensor interaction.

We would like to emphasize that the elastic scattering cross sections we have calculated here should be thought of as approximate upper limits (again, assuming no late time decays or other non-thermal mechanisms are responsible for the dark matter density). If coannihilations, resonances, or annihilations to leptons, gauge or Higgs bosons dominated the freeze-out process, then the effective couplings required to generate the observed relic abundance may be considerably smaller, leading to reduced elastic scattering cross sections with nuclei.

C. Neutrinos From WIMP Annihilations In The Sun

If WIMPs accumulate in the core of the Sun in sufficient numbers, their annihilations can potentially produce an observable flux of high-energy neutrinos [20]. WIMPs in the Solar System elastically scatter with nuclei in the Sun and become gravitationally bound at the rate approximately given by [21]

$$C_\odot \approx 3.35 \times 10^{19} \text{ s}^{-1} \left(\frac{\sigma_{\chi-p,\text{SD}} + \sigma_{\chi-p,\text{SI}} + 0.07 \sigma_{\chi-\text{He},\text{SI}}}{10^{-7} \text{ pb}} \right) \left(\frac{100 \text{ GeV}}{m_\chi} \right)^2, \quad (25)$$

where $\sigma_{\chi-p,\text{SD}}$, $\sigma_{\chi-p,\text{SI}}$ and $\sigma_{\chi-\text{He},\text{SI}}$ are the spin-dependent (SD) and spin-independent (SI) elastic scattering cross sections of WIMPs with hydrogen (protons) and helium nuclei, respectively. The factor of 0.07 reflects the solar abundance of helium relative to hydrogen and well as dynamical factors and form factor suppression.

The number of WIMP in the Sun, N , evolves as

$$\dot{N} = C_\odot - A_\odot N^2, \quad (26)$$

where A_\odot is the WIMP's annihilation cross section times the relative velocity divided by the effective volume of the Sun's core. The present annihilation rate in the Sun is given by

$$\Gamma = \frac{1}{2} A_\odot N^2 = \frac{1}{2} C_\odot \tanh^2 \left(\sqrt{C_\odot A_\odot} t_\odot \right), \quad (27)$$

where $t_\odot \approx 4.5$ billion years is the age of the solar system. The annihilation rate is maximized when it reaches equilibrium with the capture rate (*i.e.*, when $\sqrt{C_\odot A_\odot} t_\odot \gg 1$). These WIMP annihilations lead to a flux of neutrinos at Earth given by

$$\frac{dN_{\nu_\mu}}{dE_{\nu_\mu}} = \frac{C_\odot F_{\text{Eq}}}{4\pi D_{\odot-\oplus}^2} \left(\frac{dN_\nu}{dE_\nu} \right)^{\text{Inj}}, \quad (28)$$

where C_\odot is the capture rate of WIMPs in the Sun, F_{Eq} is the non-equilibrium suppression factor (approximately 1 for capture-annihilation equilibrium), $D_{\odot-\oplus}$ is the Earth-Sun distance and $(dN_\nu/dE_\nu)^{\text{Inj}}$ is the neutrino spectrum from the Sun per WIMP annihilating, which depends on the mass of the WIMP and its dominant annihilation modes. Due to $\nu_\mu - \nu_\tau$ vacuum oscillations, the muon neutrino flux observed at Earth is the average of the ν_μ and ν_τ components.

Muon neutrinos produce muons in charged current interactions with nuclei in the material inside or near the detector volume of a high-energy neutrino telescope. The rate of neutrino-induced muons observed in a high-energy neutrino telescope is given by

$$N_{\text{events}} \approx \int \int \frac{dN_{\nu_\mu}}{dE_{\nu_\mu}} \frac{d\sigma_\nu}{dy}(E_{\nu_\mu}, y) R_\mu((1-y) E_\nu) A_{\text{eff}} dE_{\nu_\mu} dy, \quad (29)$$

where $d\sigma_\nu/dy(E_{\nu_\mu}, y)$ is the neutrino-nucleon charged current interaction cross section, $(1-y)$ is the fraction of neutrino energy that goes into the muon and A_{eff} is the effective area of the detector. The factor R_μ is either the distance a muon of energy $E_\mu = (1-y) E_\nu$ travels before falling below the muon energy threshold of the experiment, called the muon range, or the width of the detector, whichever is larger. The spectrum and flux of neutrinos generated in WIMP annihilations is determined by the WIMP's mass and leading annihilation modes.

If the rate at which WIMPs are captured in the Sun is dominated by spin-independent scattering, one can translate the bounds from CDMS [17] and XENON [18] into an upper limit on the neutrino flux. In fact, even for the maximum elastic scattering cross section allowed by these experiments, no more than a few neutrino-induced muons will be generated per year in a kilometer-scale detector [22]. This is well below the sensitivity of next generation neutrino telescopes such as IceCube [23]. Thus, if we are to detect WIMP annihilations using neutrino telescopes, the capture rate must be dominated by spin-dependent scattering, which is far less constrained by direct detection experiments.

The WIMP-nucleus spin-dependent elastic scattering cross section is approximately given by [15]

$$\sigma_{\chi N} \approx \frac{32}{\pi} \frac{M_\chi^2 m_N^2}{(M_\chi^2 + m_N)^2} \Lambda^2 J(J+1), \quad (30)$$

where

$$\Lambda = \frac{1}{J} \left[\langle S_p \rangle \sum_{q=u,d,s} \frac{G_{A,q}}{2} \Delta_q^{(p)} + \langle S_n \rangle \sum_{q=u,d,s} \frac{G_{A,q}}{2} \Delta_q^{(n)} \right]. \quad (31)$$

In these expressions, J is the nuclear spin, and $\langle S_{p,n} \rangle$ are the expectation values of the spin content of protons or neutrons in the target nucleus. The quantities Δ_q are coefficients of the matrix element of the axial current in a nucleon, with values given by $\Delta_u^{(p)} = \Delta_d^{(n)} = 0.78 \pm 0.02$, $\Delta_d^{(p)} = \Delta_u^{(n)} = -0.48 \pm 0.02$, and $\Delta_s^{(p)} = \Delta_s^{(n)} = -0.15 \pm 0.02$.

Inserting these values into the above equations, the WIMP-proton, spin-dependent cross section reduces to

$$\sigma_{\chi p} \approx \frac{6 m_p^2}{\pi} [0.78 G_{A,u} - 0.48 G_{A,d} - 0.15 G_{A,s}]^2, \quad (32)$$

which, for approximately universal couplings, yields²

$$\sigma_{\chi p} \sim 10^{-7} \text{ pb} \times \left(\frac{G_{A,q}}{10^{-7} \text{ GeV}^{-2}} \right)^2. \quad (33)$$

Currently, the strongest constraints on spin-dependent WIMP-proton scattering come from the COUPP [24] and KIMS [25] collaborations, which exclude cross sections larger than $\sigma_{\chi p} \sim 10^{-1}$ pb. This limit, however, is well beyond the range anticipated for a thermal WIMP.

In Fig. 3, we plot the annihilation rate of WIMPs in the Sun for the case of a fermionic WIMP with axial couplings to quarks. To be detected over the atmospheric neutrino background, the annihilating WIMPs must generate tens of neutrino-induced muons per year in a kilometer-scale, high-energy neutrino telescope, such as IceCube. In Fig. 3 we also plot the approximate annihilation rate required to generate 20 events (above a muon threshold energy of 50 GeV) per year at IceCube. This reach is shown as solid lines for the case of WIMP annihilations to bottom quarks or gauge bosons.

² Notice that in the case of universal couplings there is an approximate cancellation of terms in Eq. (32). Departures from the universality of $G_{A,u}$, $G_{A,d}$ and $G_{A,s}$, however, could lead to larger cross sections than those estimated here. Considering the axial couplings of the Z boson to fermions, for example, the opposite signs of the couplings to up and down-type fermions leads to an elastic scattering cross section about 10^2 times larger than estimated in Eq. (33).

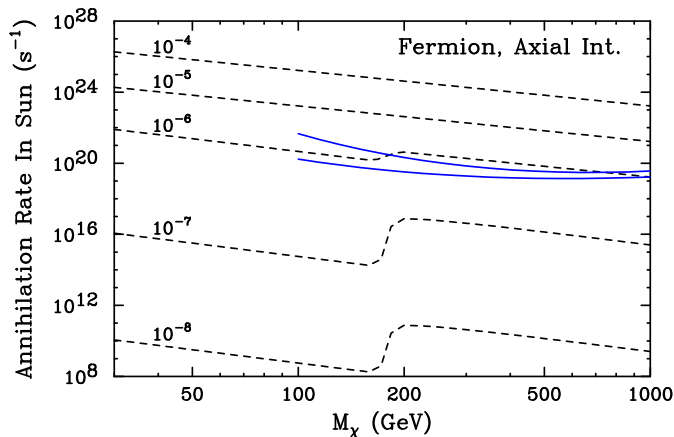


FIG. 3: The annihilation rate of WIMPs in the Sun, as a function of the WIMP’s mass, for a fermionic WIMP interacting with standard model particles through axial interactions. As before, results are given for effective couplings to each fermion species of $G_q = 10^{-8}, 10^{-7}, 10^{-6}, 10^{-5},$ and 10^{-4} GeV^{-2} . Also shown as solid lines are the approximate rates needed to be detected by an experiment such as IceCube (20 events per square kilometer, year with a 50 GeV muon energy threshold). The solid lines denote the reach for WIMPs annihilating to bottom quarks (top) or gauge bosons (bottom).

D. Indirect Searches With Gamma-Rays and Charged Particles

In addition to neutrinos, products of WIMP annihilations including gamma rays [26], electrons, positrons [27, 28], and antiprotons [28, 29] could also potentially provide detectable signals. The reach of these efforts depend on a combination of astrophysical inputs, such as the distribution of dark matter in the Galaxy and the properties of the galactic magnetic field, and on the WIMP’s properties, namely its mass, annihilation cross section, and dominant annihilation modes. Although we will not, in this article, discuss the astrophysical inputs impacting such searches, we will briefly comment on the WIMP’s annihilation cross section as it appears in our model-independent analysis.

If we fix the WIMP’s effective couplings such that its annihilation cross section at the temperature of freeze-out is equal to the value required to yield the observed dark matter abundance, then we can proceed to estimate its annihilation cross section in the low-velocity limit (the relevant limit for indirect searches). From Eqs. (13-17), we see that fermionic WIMPs annihilating through pseudoscalar, vector, and tensor interactions do so largely through terms for which σv is constant, rather than $\sigma v \propto v^2$. This leads to a low-velocity annihilation cross section of approximately $3 \times 10^{-26} \text{ cm}^3/\text{s}$ in these cases. Scalar or axial interaction forms, in contrast, lead to an annihilation cross section that scales as $\sigma v \propto v^2$, and thus imply rates suppressed by a factor of about 10^{-6} for WIMP annihilations in the Galactic halo.

E. General Conclusions for a Fermionic WIMP

Our model-independent results for a fermionic WIMP are summarized in Fig. 4. In each frame, the solid dark (black) line denotes the combinations of WIMP masses and couplings that lead to a thermal abundance of dark matter equal to the value measured by WMAP [14]. As we have pointed out, however, these calculations were performed under the assumption that resonances, coannihilations, and annihilations to gauge and Higgs bosons do not play a significant role in the thermal freeze-out process. If any of these processes have significant effects, the WIMP couplings could be considerably smaller while still producing a dark matter abundance consistent with WMAP.

Although Eqs. (6-10) do not form a complete set of Lorentz-invariant interaction Lagrangians, they are representa-

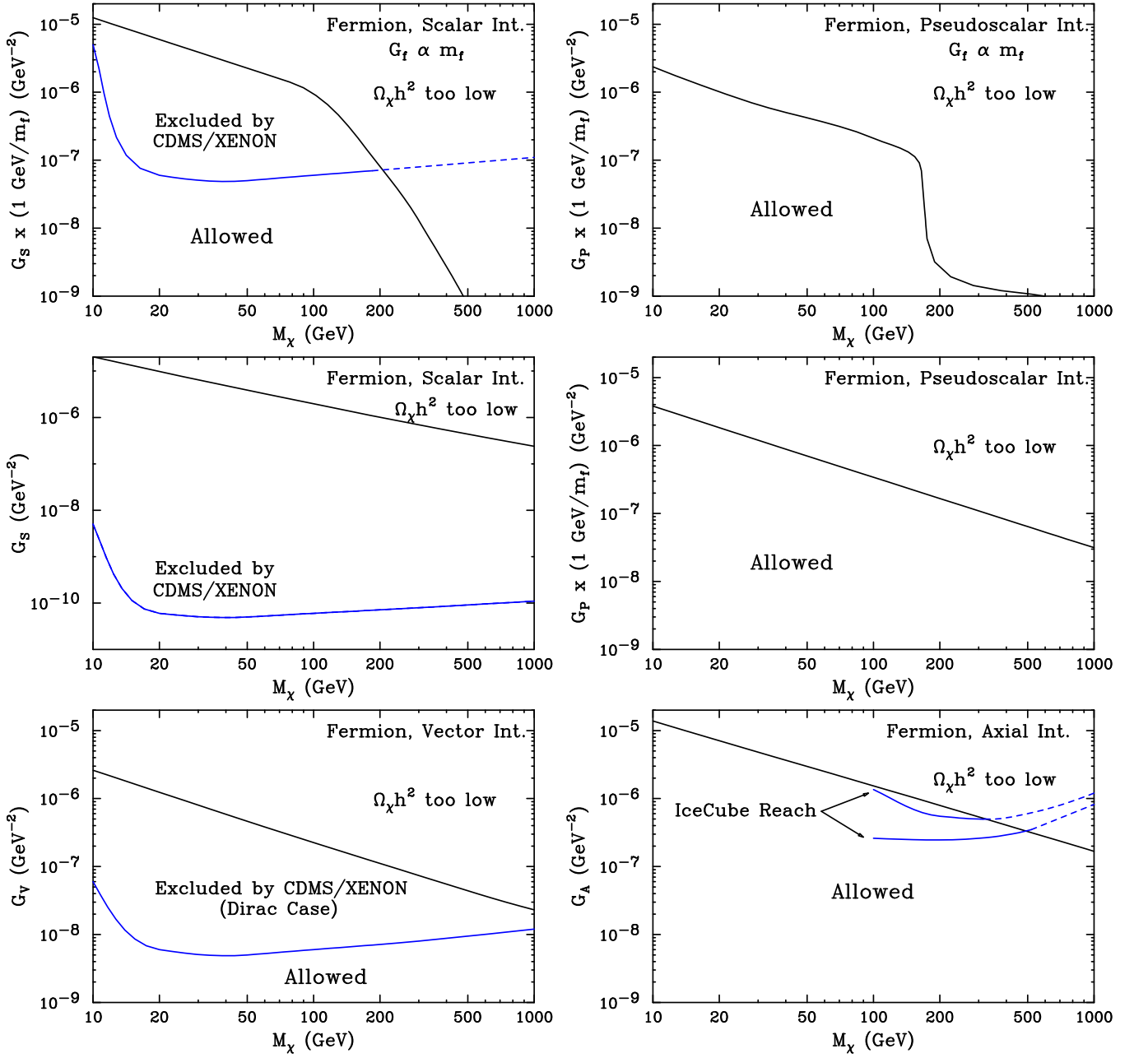


FIG. 4: A summary of the constraints on a fermionic WIMP with scalar, pseudoscalar, vector, and axial interactions, including regions excluded and allowed by direct and indirect detection experiments (note that WIMPs with pseudoscalar and axial interactions are unconstrained by direct detection experiments). If resonances, coannihilations, or annihilations to final states other than fermion-antifermion pairs are significant, smaller couplings than those shown here can lead to the measured relic abundance. See the text for more details.

tive of a larger set of combinations of interactions:

$$\text{Scalar-Pseudoscalar (SP): } \mathcal{L} = \frac{G_{SP,f}}{\sqrt{2}} \bar{\chi} \chi \bar{f} \gamma_5 f \quad (34)$$

$$\text{Pseudoscalar-Scalar (PS): } \mathcal{L} = \frac{G_{PS,f}}{\sqrt{2}} \bar{\chi} \gamma^5 \chi \bar{f} f \quad (35)$$

$$\text{Vector-Axial Vector (VA): } \mathcal{L} = \frac{G_{VA,f}}{\sqrt{2}} \bar{\chi} \gamma^\mu \chi \bar{f} \gamma_\mu \gamma_5 f \quad (36)$$

$$\text{Axial Vector-Vector (AV): } \mathcal{L} = \frac{G_{AV,f}}{\sqrt{2}} \bar{\chi} \gamma^\mu \gamma^5 \chi \bar{f} \gamma_\mu f \quad (37)$$

Up to factors of $1 - m_f^2/m_\chi^2$, WIMPs with interactions of these types will have annihilation cross sections and relic densities determined by the WIMP interaction form (the left side of the Lagrangian), and elastic scattering cross sections determined by the fermion interaction form (the right side of the Lagrangian). Consequently, interaction Lagrangians of these forms will provide results that are redundant with what we have obtained here. We will consider interaction Lagrangians of this form for scalar WIMPs, where we obtain non-redundant results.

To roughly estimate the effect of a potential resonance, consider a WIMP annihilating through the s -channel exchange of a mediator, ψ , to fermion-antifermion pairs. If $m_\psi \gg 2m_\chi$ then we can write an effective Fermi coupling, $G_f \approx \sqrt{2} \lambda_\chi \lambda_f / m_\psi^2$, where λ_χ and λ_f are the mediator's couplings to the WIMPs and final state fermions, respectively. If the mediator's mass is not much greater than twice the WIMP mass, however, the effects of the resonance on the annihilation cross section can be significant. In particular, we can roughly estimate an effective G_f for calculating the WIMP's annihilation cross section:

$$G_{f,\text{Ann}} \approx \frac{\sqrt{2} \lambda_\chi \lambda_f}{[(M_\psi^2 - 4M_\chi^2)^2 + M_\psi^2 \Gamma_\psi^2]^{1/2}}, \quad (38)$$

where Γ_ψ is the width of the mediating particle. For a 450 GeV mediator with a narrow width and a 200 GeV WIMP, the effective value of $G_{f,\text{Ann}}$ is a factor of about 5 larger than is found neglecting the effects of the resonance, which enables the measured dark matter abundance to be generated with a product of couplings (*i.e.*, $\lambda_\chi \lambda_f$) that is smaller by a factor of 5 than those shown to be required in Fig. 4. In other words, the effective value of G_f for the purposes of calculating the WIMP annihilation cross section (but not for calculating elastic scattering cross sections) is increased by a factor of 5 in this case. For the same 450 GeV mediator and a 220 GeV WIMP, the resonance enhances the effective value of G_f by a factor approximately 20. Although one should integrate the cross section over the thermal distribution to accurately account for the effect of a resonance on the relic abundance [13], we provide this estimate to illustrate how such a feature is qualitatively expected to impact the resulting dark matter density.

This effect is important in interpreting the constraints from direct detection experiments and the reach of neutrino telescopes shown in Fig. 4. Consider, for example, the case of scalar interactions with $G_f \propto m_f$ shown in the upper left frame. Although by simply comparing the dark solid line to the lighter (blue) solid line, the constraints from CDMS and XENON appear to rule out a WIMP with the measured relic abundance unless it is heavier than about 200 GeV, this conclusion can be relaxed considerably if the WIMP annihilates through a resonance. Similarly, if coannihilations or annihilations to gauge/Higgs bosons play an important role in the freeze-out process, the required effective couplings will be considerably reduced as well.

Furthermore, departures from the universality of the WIMP's couplings to fermions can also alter the results summarized here. WIMPs that couple preferentially to light (heavy) quarks will be more (less) significantly constrained by direct detection experiments and neutrino telescopes. In an extreme case, we can imagine a WIMP that annihilates almost entirely through couplings to gauge boson final states rather than fermions, which in turn would lead to highly suppressed elastic scattering cross sections.

To summarize our results for the case of a fermionic WIMP, we find:

- Fermionic WIMPs with scalar interactions are required by direct detection constraints to either 1) be heavier than about 200 GeV, 2) annihilate in the early universe through a resonance or coannihilations, or 3) couple preferentially to leptons, heavy quarks, or gauge/Higgs bosons. The case of universal couplings is very strongly disfavored by current direct detection constraints (see the middle-left frame of Fig. 4).
- The conclusions described for a fermionic WIMP with scalar interactions also apply to the case of a Dirac fermionic WIMP with vector interactions and fermionic WIMPs with tensor interactions. This is the reason why a heavy 4th generation Dirac neutrino, for example, is no longer an acceptable candidate for dark matter.

- Fermionic WIMPs with uniquely pseudoscalar or axial interactions are not constrained by direct detection experiments at this time.
- Next generation, kilometer-scale neutrino telescopes will be capable of constraining the case of fermionic WIMPs with axial interactions.

F. Neutralinos as a Case Example of a Fermionic WIMP

Departing for a moment from our model-independent analysis, we would like to comment on our results as interpreted within the context of neutralinos, which are attractive dark matter candidates in supersymmetric models [2]. Neutralinos are Majorana fermions, and undergo scalar, pseudoscalar, and axial interactions. Roughly speaking, neutralinos will be overproduced in the early universe unless at least one of the following conditions are met: 1) they are able to coannihilate efficiently with the lightest stau or other superpartners (the coannihilation region), 2) they are able to annihilate efficiently through the CP-odd Higgs boson resonance (the A -funnel region), 3) they are a strongly mixed gaugino-higgsino, leading to large couplings (the focus point region), or 4) much of the supersymmetric spectrum is relatively light, making efficient annihilations possible (the bulk region).

In the A -funnel region, neutralinos annihilate near resonance via pseudoscalar interactions, but also elastically scatter through scalar interactions associated with CP-even Higgs exchange (and squark exchange), leading to a constraint similar in form to that shown in the upper left frame of Fig. 4, but with the solid dark relic abundance contour reduced by at least one order of magnitude or more. Both the A -funnel and bulk regions are beginning to be significantly explored by direct detection experiments and, in the absence of a positive detection, will be highly constrained in the coming years.

In the focus point region, the neutralino's couplings are enhanced, leading to scalar elastic scattering cross sections near the current constraints from CDMS and XENON. Although the CDMS/XENON constraint shown in Fig. 4 is somewhat weakened by the fact that neutralino annihilations in the focus point region proceed largely to gauge boson final states, direct detection experiments will essentially close the focus point region if no detection is made in the next couple of years. Furthermore, focus point neutralinos have sizable couplings to the Z boson, leading to large spin-dependent elastic scattering cross sections through axial interactions. As mentioned before, the opposite sign of the Z 's couplings to up and down type fermions leads to a much greater reach for IceCube than is shown in the lower right frame of Fig. 4. Hundreds or thousands of events per year at IceCube are predicted throughout much of the focus point region.

Finally, neutralinos in the stau coannihilation region are the least constrained by direct and indirect searches, as their couplings can be very small without leading to their overproduction in the early universe.

III. SCALAR DARK MATTER

In this section, we consider the case of a scalar WIMP, with scalar and vector, as well as combinations of scalar/pseudoscalar and vector/axial vector, interaction forms. In analogy with Eqs. (34–5), we write

$$\text{Scalar (S): } \mathcal{L} = \frac{F_{S,f}}{\sqrt{2}} \bar{\phi} \phi \bar{f} f \quad (39)$$

$$\text{Vector (V): } \mathcal{L} = \frac{F_{V,f}}{\sqrt{2}} \bar{\phi} \overleftrightarrow{\partial}_\mu \phi \bar{f} \gamma_\mu f \quad (40)$$

$$\text{Scalar–Pseudoscalar (SP): } \mathcal{L} = \frac{F_{SP,f}}{\sqrt{2}} \bar{\phi} \phi \bar{f} \gamma_5 f \quad (41)$$

$$\text{Vector–Axial Vector (VA): } \mathcal{L} = \frac{F_{VA,f}}{\sqrt{2}} \bar{\phi} \overleftrightarrow{\partial}_\mu \phi \bar{f} \gamma_\mu \gamma_5 f, \quad (42)$$

where ϕ denotes the scalar WIMP. Note that in F_f has mass dimension of -1 for the scalar and scalar-pseudoscalar interactions, and -2 for vector and vector-axial vector interactions.

A. Scalar WIMP Annihilation and Relic Density

For scalar WIMPs, the annihilation cross sections to fermion-antifermion pairs are given by

$$\sigma_S = \frac{1}{16\pi} \sum_f F_{S,f}^2 c_f \sqrt{\frac{s-4m_f^2}{s-4M_\phi^2}} \left[\frac{(s-4m_f^2)}{s} \right] \quad (43)$$

$$\sigma_V = \frac{1}{16\pi} \sum_f F_{V,f}^2 c_f \sqrt{\frac{s-4m_f^2}{s-4M_\phi^2}} \left[\frac{2(s-4M_\phi^2)(s+2m_f^2)}{3s} \right] \quad (44)$$

$$\sigma_{SP} = \frac{1}{16\pi} \sum_f F_{SP,f}^2 c_f \sqrt{\frac{s-4m_f^2}{s-4M_\phi^2}} \quad (45)$$

$$\sigma_{VA} = \frac{1}{16\pi} \sum_f F_{VA,f}^2 c_f \sqrt{\frac{s-4m_f^2}{s-4M_\phi^2}} \left[\frac{2(s-4M_\phi^2)(s-4m_f^2)}{3s} \right] \quad (46)$$

Expanding in powers of relative velocity, we arrive at

$$\sigma_S|v| \approx \frac{1}{4\pi} \sum_f F_{S,f}^2 c_f \sqrt{1-m_f^2/M_\phi^2} \left[\frac{1}{4} \left(1 - \frac{m_f^2}{M_\phi^2} \right) \right] \quad (47)$$

$$\sigma_V|v| \approx \frac{1}{4\pi} \sum_f F_{V,f}^2 c_f M_\phi^2 \sqrt{1-m_f^2/M_\phi^2} \left[\frac{1}{3} \left(2 + \frac{m_f^2}{M_\phi^2} \right) v^2 \right] \quad (48)$$

$$\sigma_{SP}|v| \approx \frac{1}{4\pi} \sum_f F_{SP,f}^2 c_f \sqrt{1-m_f^2/M_\phi^2} \left[\frac{1}{4} \right] \quad (49)$$

$$\sigma_{VA}|v| \approx \frac{1}{4\pi} \sum_f F_{VA,f}^2 c_f M_\phi^2 \sqrt{1-m_f^2/M_\phi^2} \left[\frac{1}{3} \left(2 - \frac{m_f^2}{M_\phi^2} \right) v^2 \right]. \quad (50)$$

To calculate the thermal relic abundance of a scalar WIMP, we follow the same procedure as described in Sec. II. We show the results of this calculation in Fig. 5.

B. Direct and Indirect Detection

The calculation of the elastic scattering cross section for a scalar WIMP with nuclei is similar to that described for a fermionic WIMP in Sec. II B. Although we will not repeat the details of this calculation here, we will comment on the most important differences.

In the case of a scalar WIMP with a scalar interaction with quarks, the effective coupling F_q possesses a different dimensionality than G_q . This, in turn, leads to a stronger dependence on the WIMP mass. In particular, heavier WIMPs have a somewhat smaller elastic scattering cross section and thus are less constrained by direct detection experiments.

The elastic scattering cross sections for a scalar WIMP are shown in Fig. 6. By comparing Figs. 5 and 6, we can see that scalar interactions of the form $F_f \propto m_f$ that lead to an acceptable relic density also exceed direct detection constraints if $M_\phi \lesssim m_t$. For WIMPs heavier than the top quark, smaller couplings allow a WIMP to evade current direct detection constraints while also yielding an acceptable dark matter abundance. As in the fermionic case, we find that a scalar WIMP that annihilates largely through universal scalar couplings (equal for all fermion species) will be essentially excluded by existing direct detection constraints.

Scalar WIMPs with vector interactions are also severely constrained by present direct detection experiments. By comparing the lower frames of Figs. 5 and 6, we find that scalar WIMPs with vector interactions with fermions must be heavier than several TeV to evade current elastic scattering bounds, unless resonances, coannihilations or annihilations to gauge/Higgs bosons play an important role, in which case lighter WIMPs may also be allowed.

Spin-dependent scattering between scalar WIMPs and nuclei occurs only in the case of vector-axial vector interactions. Although the capture rate of scalar WIMPs in the Sun may potentially be large in this case, the annihilation cross section scales with v^2 (see Eq. 50), thus suppressing the annihilation rate in the Sun's core, and along with it

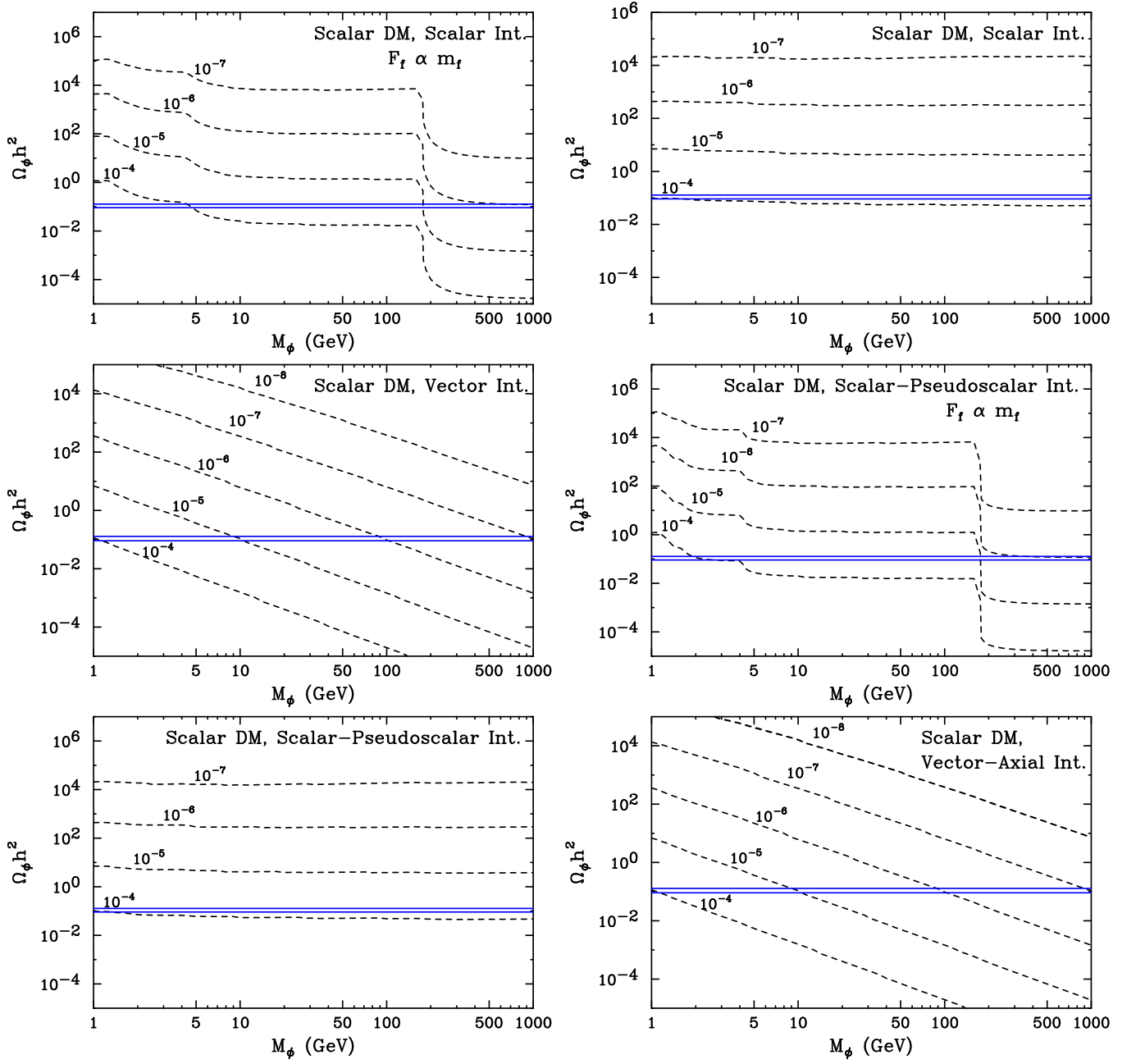


FIG. 5: The thermal relic density of scalar dark matter with scalar, vector, scalar-pseudoscalar, and vector-axial vector interactions with standard model particles. In the upper left and center right frames, results are given for effective couplings to each species of standard model fermion of $F_f \times (1 \text{ GeV}/m_f) \times (M_\psi/M_\phi) = 10^{-7}, 10^{-6}, 10^{-5},$ and 10^{-4} GeV^{-2} . In the other four frames, results for $F_f = 10^{-8}, 10^{-7}, 10^{-6}, 10^{-5},$ and 10^{-4} GeV^{-2} are given. If resonances, coannihilations, or annihilations to final states other than fermion-antifermion pairs are significant, the relic abundance is expected to be significantly lower than shown here. Also shown as horizontal lines is the range of the cold dark matter density measured by WMAP [14].

the resulting high-energy neutrino flux. Scalar WIMPs are, therefore, not expected to be within the reach of IceCube or other planned high-energy neutrino telescopes.

The prospects for the indirect detection of scalar WIMPs using gamma-rays or charged particles (e^\pm, \bar{p}) once again depend on the relationship between the WIMP's annihilation cross section and relative velocity. In the case of scalar couplings, the annihilation cross section, σv , is nearly independent of the WIMPs' relative velocity, whereas vector interactions yield $\sigma v \propto v^2$. As a result, the indirect detection prospects for a scalar WIMP with vector interactions are expected to be highly suppressed.

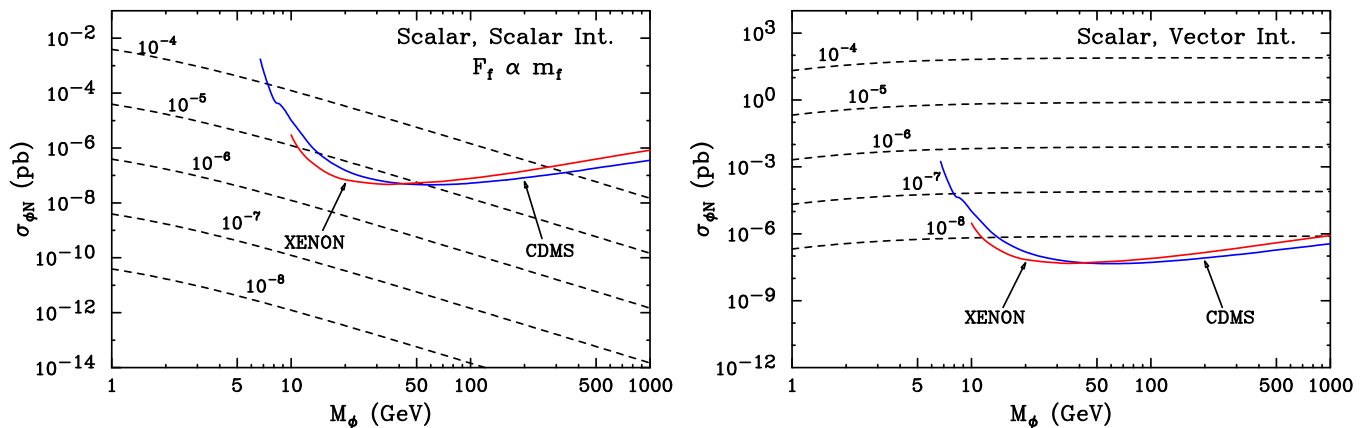


FIG. 6: The spin-independent WIMP-nucleon elastic scattering cross section as a function of WIMP mass for a scalar WIMP interacting through scalar (left) and vector (right) interactions. Results are given for effective scalar couplings to each quark species of $F_q \times (1 \text{ GeV}/m_q) = 10^{-8}, 10^{-7}, 10^{-6}, 10^{-5},$ and 10^{-4} GeV^{-2} and for effective vector couplings to each quark of $F_q = 10^{-8}, 10^{-7}, 10^{-6}, 10^{-5},$ and 10^{-4} GeV^{-2} . Also shown as solid curves are the current upper limits from the CDMS [17] and XENON [18] experiments. We do not show the case in which the scalar couplings are equal for each quark species, as its leads to much larger cross sections and are strongly excluded.

C. General Conclusions for a Scalar WIMP

Our model-independent results for a scalar WIMP are summarized in Fig. 7. In each frame, the solid dark (black) line denotes the combinations of WIMP mass and couplings that lead to a thermal abundance equal to the measured dark matter density, again in the absence of significant effects of resonances, coannihilations, or annihilations to gauge/Higgs bosons. The lighter (blue) curve in each frame denotes the current constraints from the direct detection experiments CDMS and XENON.

To summarize our results for the case of a scalar WIMP, we find:

- Scalar WIMPs with scalar interactions with standard model fermions are required by direct detection constraints to 1) be heavier than about 80 GeV, 2) annihilate in the early universe through a resonance or coannihilations, or 3) couple preferentially to leptons, heavy quarks, or gauge/Higgs bosons. The case of universal couplings is very strongly disfavored by current direct detection constraints (see the upper-right frame of Fig. 7).
- The conditions described for a scalar WIMP with scalar interactions also apply to the case of a scalar WIMP with vector interactions. In the absence of resonances, coannihilations, and/or annihilations to gauge/Higgs bosons, current direct detection constraints exclude such a dark matter candidate by multiple orders of magnitude.
- Neutrino telescopes are not likely to constrain scalar WIMPs beyond the level already achieved by direct detection experiments.

IV. SUMMARY AND CONCLUSIONS

Even if the Large Hadron Collider does not reveal physics beyond the standard model, a dark matter candidate in the form of a weakly interacting massive particle may still exist. In this article, we have studied how the nature of such a WIMP could be deduced by its signatures in astrophysical experiments. In our analysis, we have taken a general and model-independent approach, considering fermionic or scalar WIMPs with a variety of interaction forms.

In Table I, we summarize our findings. For each combination of spin and interaction form, we indicate the constraints placed by and the prospects for direct detection experiments, high-energy neutrino telescopes, and indirect detection experiments using gamma-rays or charged particles. Under the column of direct detection, we use the phrases “strongly excluded,” “weakly excluded,” or “within near future reach,” to denote the sensitivity or prospects for each case. By “strongly excluded,” we indicate instances in which the effective couplings to quarks, as relevant to elastic scattering with nuclei, must be suppressed by more than a factor of ten relative to the value required to generate thermally the observed dark matter abundance. As we have discussed, such a suppression could result from resonant annihilations, coannihilations, or annihilations to gauge/Higgs bosons. The label “weakly excluded,” in contrast, indicates only that

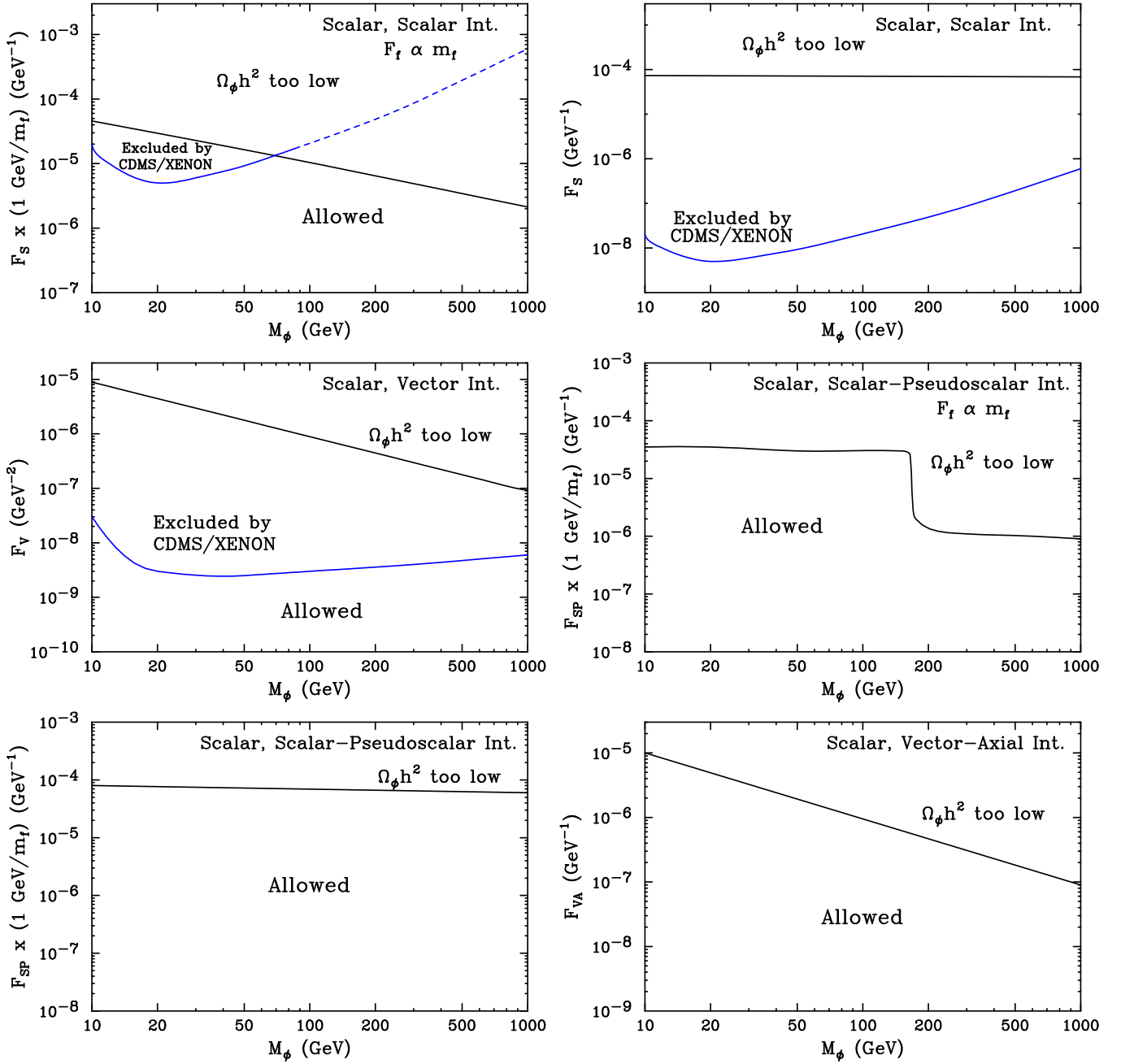


FIG. 7: A summary of the constraints on a scalar WIMP with scalar or vector interactions. If resonances, coannihilations, or annihilations to final states other than fermion-antifermion pairs are significant, smaller couplings than those shown here can lead to the measured relic abundance. See the text for more details.

the case is excluded if the effective couplings to quarks are not suppressed by such effects. Lastly, the label “within near-future reach” indicates an elastic scattering cross section (without suppression) that is within approximately two orders of magnitudes of current direct detection limits.

Under the column of neutrino telescopes, we classify each case as either not sensitive or sensitive over a range of WIMP masses (for next generation experiments, such as IceCube). This evaluation depends on the annihilation products of the WIMP, however, and thus are highly approximate. Under the column of gamma-rays and charged cosmic rays, we simply indicate whether the WIMP’s annihilations are or are not suppressed by the square of the WIMP’s velocity. If such velocity suppression is present, it is highly unlikely that GLAST, PAMELA or other planned indirect detection experiments will be capable of detecting dark matter.

This leads us to the most obvious and important question: Will the information provided by direct and indirect

detection experiments be able to be used to infer the particle nature of the dark matter? Although there are certainly cases in which measurements by these experiments will not lead to an unambiguous identification, there are many scenarios in which a great deal could be learned. For example, if IceCube or another high-energy neutrino telescope were to observe neutrinos from WIMP annihilations in the Sun, we would be able to conclude that the WIMP is likely fermionic,³ and that it possesses an axial interaction with light quarks. By studying the precise rate observed, one could also potentially determine whether the WIMP’s axial interaction played a dominant or only subdominant role in the process of thermal freeze-out. This could be combined with observations from direct detection experiments to further constrain the possible interactions possessed by the WIMP.

As a second possible scenario, imagine that near future direct detection experiments observe a WIMP with a mass of a few hundred GeV and that, shortly afterward, GLAST observes a corresponding gamma-ray signal from WIMPs annihilating in the halo. From Table I, we can see that this leads us to only three likely possibilities: the WIMP is either a fermion with vector interactions, a fermion with pseudoscalar-scalar interactions, or a scalar with Yukawa-like scalar interactions.

Although previous studies have shown that dark-matter experiments have the potential to constrain the parameters of supersymmetry [33] or even to help identify the theoretical framework from which the dark matter arises [34], here we have demonstrated that a far more model-independent approach can also be fruitful. In particular, without assuming any particular theoretical framework or model, we have shown that direct and indirect dark matter experiments can be used to considerably constrain the spin and interactions of the dark matter, even in the absence of any discoveries at the LHC.

The results presented in Table I rely upon the set of assumptions we have adopted. It must be noted that if dark matter consists of non-thermally produced WIMPs, or of multiple species of particles, our conclusions could be altered considerably. Furthermore, one might worry that the effects of resonances, coannihilations, or annihilations to gauge/Higgs bosons, which we have largely neglected in our analysis, might dramatically change our conclusions. To some degree, however, the impact of such processes are encapsulated in our definitions of “strongly excluded” and “weakly excluded”, as used in Table I. For example, if a WIMP annihilates largely through a narrow resonance such that twice the mass of the WIMP lies within approximately 5% of the exchanged particle, then the effective couplings relevant for elastic scattering can be reduced by a factor of ten without the WIMP being overproduced in the early universe (see Sec. II E). This mildly (5% or less) fine-tuned resonance corresponds to the “weakly excluded” label used in the table. Anything labeled “strongly excluded” would require the masses to be tuned even more precisely to the resonance value to remain viable. Similarly, if a significant fraction of WIMP annihilations in the early universe proceeded to a combination of gauge or Higgs bosons, or occurred through coannihilations with another species of particle, the elastic scattering cross section could be suppressed. For the scenarios we have labeled as “strongly excluded” to have remained hidden from direct detection experiments, however, about 99% or more of the annihilations/coannihilations of WIMPs in the early universe must have occurred through such processes. So although the conclusions we have reached here are not entirely immune to the inclusion of such effects, they are quite robust in all but the most extreme cases.

In conclusion, we find that in the case that the Large Hadron Collider does not discover physics beyond the standard model, astrophysical experiments may still be able to constrain the nature of the dark matter, even without assuming supersymmetry or any other specific particle physics framework. In particular, the spin and interaction forms of dark matter can potentially be identified by combining results from direct detection experiments, neutrino telescopes, and indirect detection experiments using gamma-rays or charged cosmic rays.

Acknowledgments

We would like to thank Rakhi Mahbubani, Keith Olive, and Pearl Sandick for illuminating discussions. DH is supported by the Fermi Research Alliance, LLC under Contract No. DE-AC02-07CH11359 with the US Department

³ More precisely, we could conclude in this case that the dark matter particle is not a scalar. Vector WIMPs, which we have not studied in this paper, could also potentially generate an observable flux of high-energy neutrinos [32].

Fermionic Dark Matter

| Interaction | Direct Detection | Neutrino Telescopes | γ -rays, e^\pm , \bar{p} |
|--|--|---------------------------------------|-------------------------------------|
| Scalar ($G_f \propto m_f$) | Strongly Excluded $M_\chi \approx 10 - 100$ GeV Weakly Excluded $M_\chi \approx 100 - 200$ GeV Within Near Future Reach $M_\chi \approx 200 - 300$ GeV | Not Sensitive | Suppressed by v^2 |
| Scalar (G_f Universal) | Strongly Excluded $M_\chi \approx 10$ GeV–10 TeV | NA | Suppressed by v^2 |
| Pseudoscalar | Not Sensitive | Not Sensitive | Unsuppressed |
| Vector/Tensor | Strongly Excluded $M_\chi \approx 10 - 350$ GeV Weakly Excluded $M_\chi \approx 350$ GeV–2 TeV | Not Sensitive | Unsuppressed |
| Axial | Not Sensitive | Sensitive $M_\chi \sim 100 - 500$ GeV | Suppressed by v^2 |
| Scalar-Pseudoscalar | Not Sensitive | Not Sensitive | Suppressed by v^2 |
| Pseudoscalar-Scalar ($G_f \propto m_f$) | Weakly Excluded $M_\chi \approx 10 - 180$ GeV Within Near Future Reach $M_\chi \approx 180 - 800$ GeV | Not Sensitive | Unsuppressed |
| Vector-Axial | Not Sensitive | Not Sensitive | Unsuppressed |
| Axial-Vector | Strongly Excluded $M_\chi \approx 10$ GeV–2 TeV Weakly Excluded $M_\chi \approx 2 - 10$ TeV | Not Sensitive | Unsuppressed |

Scalar Dark Matter

| Interaction | Direct Detection | Neutrino Telescopes | γ -rays, e^\pm , \bar{p} |
|---------------------------------|--|---------------------|-------------------------------------|
| Scalar ($F_f \propto m_f$) | Weakly Excluded $M_\phi \approx 10 - 70$ GeV Within Near Future Reach $M_\phi \approx 70 - 200$ GeV | Not Sensitive | Unsuppressed |
| Scalar (F_f Universal) | Strongly Excluded $M_\phi \approx 10$ GeV–10 TeV | NA | Unsuppressed |
| Vector | Strongly Excluded $M_\phi \approx 10$ GeV–1 TeV Weakly Excluded $M_\phi \approx 1 - 5$ TeV | Not Sensitive | Suppressed by v^2 |
| Scalar-Pseudoscalar | Not Sensitive | Not Sensitive | Unsuppressed |
| Vector-Axial | Not Sensitive | Not Sensitive | Suppressed by v^2 |

TABLE I: A summary of our results, describing the sensitivity and prospects for the direct and indirect detection of dark matter particles in the various cases we have considered. See the text for explanations for the labels used.

of Energy and by NASA grant NNX08AH34G.

-
- [1] G. Bertone, D. Hooper and J. Silk, Phys. Rept. **405**, 279 (2005).
[2] H. Goldberg, Phys. Rev. Lett. **50**, 1419 (1983); J. R. Ellis, J. S. Hagelin, D. V. Nanopoulos, K. A. Olive and M. Srednicki, Nucl. Phys. B **238**, 453 (1984); G. L. Kane, C. F. Kolda, L. Roszkowski and J. D. Wells, Phys. Rev. D **49**, 6173 (1994) [arXiv:hep-ph/9312272].
[3] E. W. Kolb and R. Slansky, Phys. Lett. B **135**, 378 (1984); H. C. Cheng, J. L. Feng and K. T. Matchev, Phys. Rev. Lett. **89**, 211301 (2002) [arXiv:hep-ph/0207125]; D. Hooper and S. Profumo, Phys. Rept. **453**, 29 (2007) [arXiv:hep-ph/0701197].
[4] G. Servant and T. M. P. Tait, Nucl. Phys. B **650**, 391 (2003) [arXiv:hep-ph/0206071];
[5] K. Agashe and G. Servant, Phys. Rev. Lett. **93**, 231805 (2004) [arXiv:hep-ph/0403143]; JCAP **0502**, 002 (2005) [arXiv:hep-ph/0411254]; K. Agashe, A. Falkowski, I. Low and G. Servant, arXiv:0712.2455 [hep-ph].
[6] H. C. Cheng and I. Low, JHEP **0408**, 061 (2004) [arXiv:hep-ph/0405243]; I. Low, JHEP **0410**, 067 (2004) [arXiv:hep-ph/0409025]; A. Birkedal, A. Noble, M. Perelstein and A. Spray, Phys. Rev. D **74**, 035002 (2006) [arXiv:hep-ph/0603077].
[7] A. Birkedal, K. Matchev and M. Perelstein, Phys. Rev. D **70**, 077701 (2004) [arXiv:hep-ph/0403004].

- [8] J. L. Feng, S. Su and F. Takayama, *Phys. Rev. Lett.* **96**, 151802 (2006) [arXiv:hep-ph/0503117].
- [9] F. Giuliani, *Phys. Rev. Lett.* **93**, 161301 (2004) [arXiv:hep-ph/0404010].
- [10] A. Kurylov and M. Kamionkowski, *Phys. Rev. D* **69**, 063503 (2004) [arXiv:hep-ph/0307185].
- [11] P. Gondolo and G. Gelmini, *Nucl. Phys. B* **360**, 145 (1991).
- [12] E. W. Kolb and M. S. Turner, *Front. Phys.* **69**, 1 (1990);
- [13] K. Griest and D. Seckel, *Phys. Rev. D* **43**, 3191 (1991).
- [14] E. Komatsu *et al.* [WMAP Collaboration], arXiv:0803.0547 [astro-ph].
- [15] G. Jungman, M. Kamionkowski and K. Griest, *Phys. Rept.* **267**, 195 (1996)
- [16] J. R. Ellis, A. Ferstl and K. A. Olive, *Phys. Lett. B* **481**, 304 (2000)
- [17] Z. Ahmed *et al.* [CDMS Collaboration], arXiv:0802.3530 [astro-ph].
- [18] J. Angle *et al.* [XENON Collaboration], *Phys. Rev. Lett.* **100**, 021303 (2008) [arXiv:0706.0039 [astro-ph]].
- [19] F. Halzen and A. D. Martin, *New York, Usa: Wiley (1984) 396p.*
- [20] L. Bergstrom, J. Edsjo and P. Gondolo, *Phys. Rev. D* **55**, 1765 (1997) [arXiv:hep-ph/9607237]; *Phys. Rev. D* **58**, 103519 (1998) [arXiv:hep-ph/9806293]; V. D. Barger, F. Halzen, D. Hooper and C. Kao, *Phys. Rev. D* **65**, 075022 (2002).
- [21] A. Gould, *Astrophys. J.* **388**, 338 (1991).
- [22] F. Halzen and D. Hooper, *Phys. Rev. D* **73**, 123507 (2006) [arXiv:hep-ph/0510048].
- [23] T. DeYoung [IceCube Collaboration], *Int. J. Mod. Phys. A* **20**, 3160 (2005); J. Ahrens *et al.* [The IceCube Collaboration], *Nucl. Phys. Proc. Suppl.* **118**, 388 (2003) [arXiv:astro-ph/0209556].
- [24] E. Behnke *et al.* [COUPP Collaboration], *Science* **319**, 933 (2008) [arXiv:0804.2886 [astro-ph]].
- [25] H. S. Lee. *et al.* [KIMS Collaboration], *Phys. Rev. Lett.* **99**, 091301 (2007) [arXiv:0704.0423 [astro-ph]].
- [26] L. Bergstrom, P. Ullio and J. H. Buckley, *Astropart. Phys.* **9**, 137 (1998) [arXiv:astro-ph/9712318]; P. Ullio, L. Bergstrom, J. Edsjo and C. G. Lacey, *Phys. Rev. D* **66**, 123502 (2002) [arXiv:astro-ph/0207125]; S. Dodelson, D. Hooper and P. D. Serpico, *Phys. Rev. D* **77**, 063512 (2008) [arXiv:0711.4621 [astro-ph]]; E. A. Baltz *et al.*, *JCAP* **0807**, 013 (2008) [arXiv:0806.2911 [astro-ph]].
- [27] E. A. Baltz and J. Edsjo, *Phys. Rev. D* **59** (1999) 023511 [arXiv:astro-ph/9808243]; D. Hooper and J. Silk, *Phys. Rev. D* **71**, 083503 (2005) [arXiv:hep-ph/0409104].
- [28] S. Profumo and P. Ullio, *JCAP* **0407**, 006 (2004) [arXiv:hep-ph/0406018];
- [29] L. Bergstrom, J. Edsjo and P. Ullio, *Astrophys. J.* **526**, 215 (1999) [arXiv:astro-ph/9902012]; A. Bottino, F. Donato, N. Fornengo and P. Salati, *Phys. Rev. D* **58**, 123503 (1998) [arXiv:astro-ph/9804137]; T. Bringmann and P. Salati, *Phys. Rev. D* **75**, 083006 (2007) [arXiv:astro-ph/0612514].
- [30] C. Arina and N. Fornengo, *JHEP* **0711**, 029 (2007) [arXiv:0709.4477 [hep-ph]]; T. Falk, K. A. Olive and M. Srednicki, *Phys. Lett. B* **339**, 248 (1994) [arXiv:hep-ph/9409270].
- [31] B. A. Dobrescu, D. Hooper, K. Kong and R. Mahubani, *JCAP* **0710**, 012 (2007) [arXiv:0706.3409 [hep-ph]].
- [32] D. Hooper and G. D. Kribs, *Phys. Rev. D* **67**, 055003 (2003) [arXiv:hep-ph/0208261].
- [33] E. A. Baltz, M. Battaglia, M. E. Peskin and T. Wizansky, *Phys. Rev. D* **74**, 103521 (2006) [arXiv:hep-ph/0602187]; D. Hooper and A. M. Taylor, *JCAP* **0703**, 017 (2007) [arXiv:hep-ph/0607086]; B. Altunkaynak, M. Holmes and B. D. Nelson, arXiv:0804.2899 [hep-ph]; D. Hooper and L. T. Wang, *Phys. Rev. D* **69**, 035001 (2004) [arXiv:hep-ph/0309036].
- [34] D. Hooper and G. Zaharijas, *Phys. Rev. D* **75**, 035010 (2007) [arXiv:hep-ph/0612137]; G. Bertone, D. G. Cerdeno, J. I. Colgar and B. C. Odom, *Phys. Rev. Lett.* **99**, 151301 (2007) [arXiv:0705.2502 [astro-ph]].